

Proton transfer dynamics of the reaction $\text{H}_3\text{O}^+(\text{NH}_3, \text{H}_2\text{O})\text{NH}_4^+$ studied using the crossed molecular beam technique

Yue Li and James M. Farrar^{a)}

Department of Chemistry, University of Rochester, Rochester, New York 14627

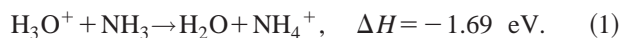
(Received 29 September 2003; accepted 8 October 2003)

The proton transfer reaction of H_3O^+ and NH_3 was studied using the crossed molecular beam technique at relative energies of 0.41, 0.81, and 1.27 eV. At all three energies, the center-of-mass flux distribution of the product ion NH_4^+ exhibits sharply asymmetry, and the maximum is close to the velocity and direction of the precursor ammonia beam. The reaction transforms almost all of the 1.69 eV exothermicity into internal excitation of the products at all three collision energies. At the lowest collision energy of 0.41 eV, nearly 77% of the total energy appears in NH_4^+ internal excitation. However, almost 100% of the incremental translational energy in the two higher-energy experiments appears in the product translational energy. Such an observation provides a classic example of the “induced repulsive energy release” mechanism that is expected to be operative on the highly skewed potential energy surfaces characteristic of the heavy+light-heavy mass combination. These results indicate that the proton transfer proceeds through a direct reaction mechanism; a Rice–Ramsperger–Kassel–Marcus theory calculation shows that the lifetime of the intermediate complex $[\text{NH}_3\text{–H–H}_2\text{O}]^+$ is about 100 fs. Proton transfer occurs early on the reaction coordinate, when the incipient N–H bond is extended, and results in highly vibrationally excited NH_4^+ products, with excitation primarily in N–H stretching modes. © 2004 American Institute of Physics. [DOI: 10.1063/1.1630312]

I. INTRODUCTION

Proton transfer in hydrogen-bonded systems is a fundamental process in nature. The investigations of proton transfer reaction mechanisms are important for understanding many basic biological, physical, and chemical processes such as solvation, photosynthesis, acid-base neutralization, and enzymatic reactions.^{1,2} Water and ammonia are both small molecules that can form hydrogen bonds because they contain the oxygen or nitrogen atom of high electronegativity, respectively. The reactions between hydronium ions and water or ammonia are simple, prototypical systems for studying the proton transfer phenomenon and have therefore long attracted the attentions of scientists.^{3–7}

The proton transfer reaction between the protonated water ion and ammonia, reaction (1), is highly exothermic. The reaction enthalpy can be simply given by the difference in the proton affinities (PA) of ammonia and water [$\text{PA}(\text{NH}_3) = 8.85$ eV, $\text{PA}(\text{H}_2\text{O}) = 7.16$ eV (Ref. 8)],



In the photoionization of ammonia and water binary clusters,⁹ the dominant products are the protonated $(\text{NH}_3)_n(\text{H}_2\text{O})_m\text{H}^+$ ions, the products of intracluster proton transfer reactions. Chang *et al.*¹⁰ measured the infrared vibrational predissociation spectra of $\text{NH}_4^+(\text{H}_2\text{O})_n$ ($n = 2 \rightarrow 7$). These results indicate that the H_3O^+ and NH_3 subunits can form stable hydrogen-bonded complexes. The structure and energy of the $[\text{NH}_3\text{–H–H}_2\text{O}]^+$ complex have

been calculated at several different levels of theory.^{11–18} These *ab initio* calculations and the experimental results based on high-pressure mass spectrometry^{19–21} show that the dissociation energy of the complex is about 0.9 eV relative to the $\text{NH}_4^+ + \text{H}_2\text{O}$ channel. The potential energy surface of the complex is sensitive to the distance between the oxygen and nitrogen atoms. At the equilibrium $R(\text{N–O})$ bond length, the potential energy surface only contains a single well corresponding to $[\text{H}_3\text{NH}\cdots\text{OH}_2]^+$, in which the central proton is more closely associated with NH_3 ; that is, the complex looks more like a complex of NH_4^+ and H_2O , rather than H_3O^+ and NH_3 . As the distance between the two atoms is increased, the barrier appears and the potential energy surface has two wells, corresponding to $[\text{H}_3\text{NH}\cdots\text{OH}_2]^+$ and $[\text{H}_3\text{N}\cdots\text{HOH}_2]^+$. At the MP2/6-31G(*d,p*) level, the barrier is 0.04 eV at $R(\text{N–O}) = 2.9$ Å and increases to 0.85 eV at 3.4 Å.¹⁵

Based on an *ab initio* calculation of the potential energy surface,^{15,22} Bueker *et al.* studied the trajectories of the proton transfer reaction (1). They concluded that the lifetime of the intermediate ion–molecule complex formed upon encounter of reactants depends strongly on their initial relative orientation. When the proton to be transferred is properly lined up between oxygen and nitrogen, rapid transfer occurs. This leads to deposition of a high and nonstatistical fraction of the reaction enthalpy into the product ammonium ion. Less favorable initial orientations appear to give a more statistical energy distribution. Cheng²³ studied the dynamics of clusters $(\text{H}_2\text{O})_n\text{H}^+$ ($n = 1–4$) interacting with an NH_3 mol-

^{a)} Author to whom correspondence should be addressed. Electronic mail: farrar@chem.rochester.edu

ecule by first-principles Born–Oppenheimer molecular dynamics simulations. He found that the transfer reaction is a rather fast process ($t=100\text{--}300$ fs). After the transfer process, the NH_4^+ ion is vibrationally hot because of the released potential energy.

Experimentally, Smith *et al.*²⁴ used a selected ion flow tube apparatus to study the binary reactions of $(\text{H}_2\text{O})_n\text{H}^+$ ($n=1\text{--}3$) ions and their deuterated analogues with NH_3 . They found that no appreciable isotopic exchange occurred and thus suggested that the reactions proceeded via the simple mechanisms of D^+ (or H^+) transfer; any intermediate complex has such a short lifetime that scrambling could not occur. A similar conclusion was also obtained by Honma *et al.*,²⁵ who studied the reaction of protonated water clusters with deuterated ammonia using guided ion beam mass spectrometry. Because the NH_2D_2^+ or DH_2O^+ ions, the H/D randomization products, were not observed as a primary product, they suggested that the reactions proceed via a direct proton transfer or via a relatively short-lived intermediate.

So far, no crossed beam experimental results have been reported for this system. In this paper, we report the results obtained using the crossed molecular beam technique, by which the initial kinetic energies and directions of the reactants can be well controlled and the angular and kinetic energy distributions of the product ions can be precisely measured. Thus more detailed information on the reaction dynamics can be extracted. This study can help us answer the following questions: (i) What is the mechanism of proton transfer? Is the proton transferred via a long-lived intermediate complex or as a direct process? (ii) How is the large exothermicity partitioned in the degrees of freedom of the products?

II. EXPERIMENT

The experimental apparatus has been described in detail in a previous paper,²⁶ so only a brief overview is provided here. The H_3O^+ ions were produced using electron impact on a room-temperature water and hydrogen mixture. The pressure in the ion source is typically 5×10^{-5} Torr. The ions are then mass selected with a 60° magnetic sector. After deceleration to the desired beam energy and focusing by a series of ion optics, the beam has a full width at half maximum (FWHM) of 0.25–0.40 eV. The ammonia beam was formed by supersonic expansion of the pure gas through a 0.07-mm nozzle. A 1.0-mm-diam skimmer, located 50 nozzle diameters downstream from the nozzle, selects the cool core of the beam. The beam enters a differential pumping chamber, where it is collimated with a 3.0-mm² aperture located approximately 2.5 cm from the skimmer, before entering the main chamber, where it intersects with the ion beam at a 90° angle. A tuning fork chopper modulates the beam at 30 Hz to provide the synchronization for the experiment. The most probable velocity of the neutral beam formed through supersonic expansion is calculated using

$$V_{\text{peak}} = \sqrt{\frac{2kT}{m} \left(\frac{\gamma}{\gamma-1} \right)}, \quad (2)$$

in which γ , the ratio of heat capacities, is 1.33 for ammonia. A rotatable electrostatic energy analyzer with a laboratory resolution of 0.07 eV was used to measure the kinetic energies of ions in the primary ion beam and scattered ionic reaction products. The ions were mass selected with a quadrupole mass spectrometer and were detected with a dual-microchannel-plate ion detector. Data were collected with a computer-controlled multichannel scalar synchronized with the beam modulation. The energy analyzer was calibrated before and after the experiments. The resonant charge transfer reaction between He^+ and He was used as the calibration reaction to determine the zero offset of the energy analyzer.

In the experiments, two independent measurements were performed: First, by rotating the angle of the energy analyzer, one can measure the relative angular distribution of product ions in the laboratory coordinate system. Second, the kinetic energy distributions of the scattered product ions can be also measured at fixed (15–20) laboratory angles. Each energy spectrum consists of 80 points, with typical energy bin widths of 0.025 eV. The two measurements result in data sets consisting of approximately 1200 data points covering laboratory velocity space.

III. DATA ANALYSIS

The aim of the data analysis procedure is to recover center-of-mass reaction differential cross sections $I_{\text{c.m.}}(u, \theta)$ from the laboratory data. In the experiments, the ion and neutral beams have velocity and angular spreads. These result in distributions of collision energies and intersection angles. In the data analysis, these distributions must be taken into account when transforming the laboratory flux distributions to the center-of-mass cross sections. This procedure was accomplished with a pointwise iterative deconvolution procedure using²⁷

$$I_{\text{lab}}(v, \Theta) = \sum_{i=1}^N f_i \frac{v^2}{u_i^2} I_{\text{c.m.}}(u_i, \theta_i). \quad (3)$$

Five points are used to represent the energy distributions of each of the two reagent beams, and five points represent the intersection angle distribution; thus, in the above equation, N is 125. f_i is a weighing factor, which is the probability of observing Newton diagram i based on the reagent beam distributions. Using the derived $I_{\text{c.m.}}(u, \theta)$, the deconvolution procedure also calculates the angular distributions and kinetic energy distributions at each angle in the laboratory coordinate. The comparison between the simulated and experimental results provides a figure of merit for the deconvolution process. In this study, the errors of the simulations are less than 6%.

Using the derived $I_{\text{c.m.}}(u, \theta)$, the barycentric angular distribution $g(\theta)$ of the products can be calculated by integrating over product translational energy. $g(\theta)$ represents the relative intensities of products scattered into center-of-mass scattering angle θ averaged over product kinetic energy. In practice, it is calculated by replacing the integral with a summation,

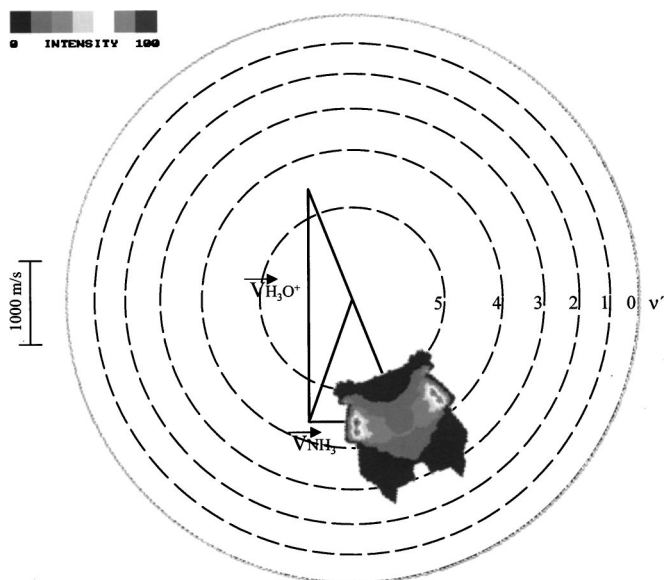


FIG. 1. Newton diagram and scattered product contour map of the proton transfer reaction $\text{H}_3\text{O}^+ + \text{NH}_3 \rightarrow \text{H}_2\text{O} + \text{NH}_4^+$ at the relative energy of 0.41 eV.

$$g(\theta) = \sum_i^M I_{\text{c.m.}}(u_i, \theta), \quad (4)$$

in which M represents the number of recoil energies considered. Similarly, the angle-averaged relative translational energy distribution of products, $P(E_T')$, can be calculated using

$$P(E_T') = \sum_i^L I_{\text{c.m.}}(u, \theta_i) \frac{\sin \theta_i}{u}. \quad (5)$$

IV. RESULTS AND DISCUSSION

The experiments were performed at selected center-of-mass collision energies of 0.41, 0.81, and 1.27 eV. These correspond to ion beams with laboratory energies of 0.74, 1.61, and 2.57 eV, respectively. According to the measured kinetic energy of the reactant ions and the calculated velocity of the neutral beam using Eq. (2), the Newton diagrams of the three energies are obtained, as shown in Figs. 1–3. In the figures, 0° is defined as the direction of the H_3O^+ ion beam in laboratory coordinates, while 90° is the direction of the neutral beam. The polar flux contour maps in the center-of-mass coordinate system, which are obtained with the deconvolution procedure, are superimposed on the Newton diagrams.

It can be seen from Figs. 1–3 that at all the collision energies, the flux distributions are sharply asymmetric and the maxima are near 180° . This observation indicates that the NH_4^+ ion has nearly the same direction as the precursor ammonia beam, a characteristic of direct reactions. Therefore, the reactions take place through large impact parameters, resulting in little change of momentum of the NH_3 unit after proton transfer. Any intermediate complex in the reactions must be short lived, because if its lifetime were on the

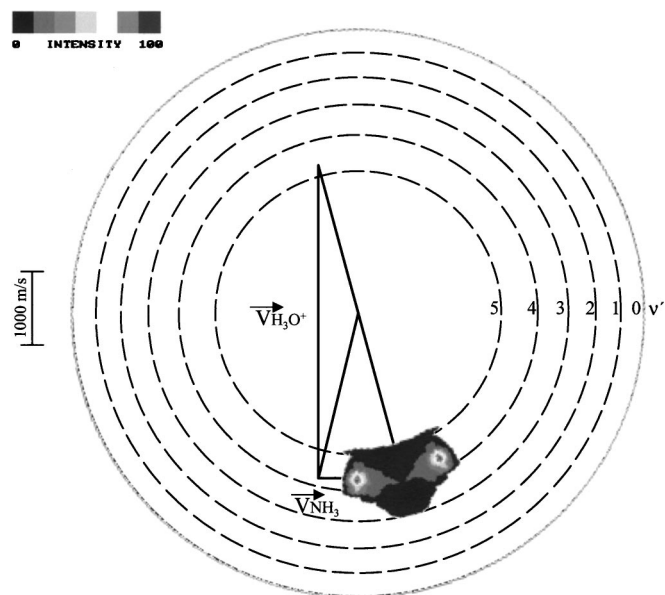


FIG. 2. Newton diagram and scattered product contour map of the proton transfer reaction $\text{H}_3\text{O}^+ + \text{NH}_3 \rightarrow \text{H}_2\text{O} + \text{NH}_4^+$ at the relative energy of 0.81 eV.

order of a rotational period or longer, one would expect to see symmetry in the scattered ion distributions with respect to the backward and forward directions.

In the experiments, only a limited range of laboratory angles (-2° – 112°) can be measured; this results in the loss of flux at angles close to 180° in the center-of-mass coordinate. Consequently, the center-of-mass angular distributions of the product ions shown in Fig. 4(a) appear to peak at a slightly smaller angle, but not at 180° .

Figure 4(b) shows the relative translational energy distributions of the products, $P(E_T')$, at the three experimental energies. It can be seen from Fig. 4(b) that as the collision

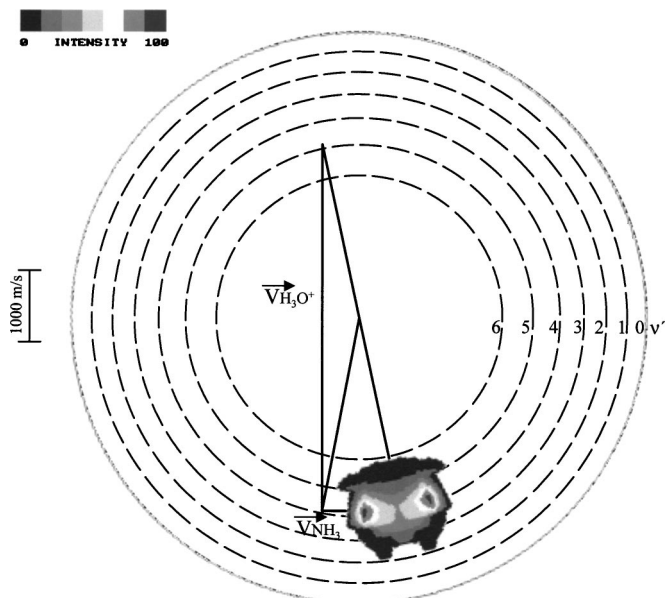


FIG. 3. Newton diagram and scattered product contour map of the proton transfer reaction $\text{H}_3\text{O}^+ + \text{NH}_3 \rightarrow \text{H}_2\text{O} + \text{NH}_4^+$ at the relative energy of 1.27 eV.

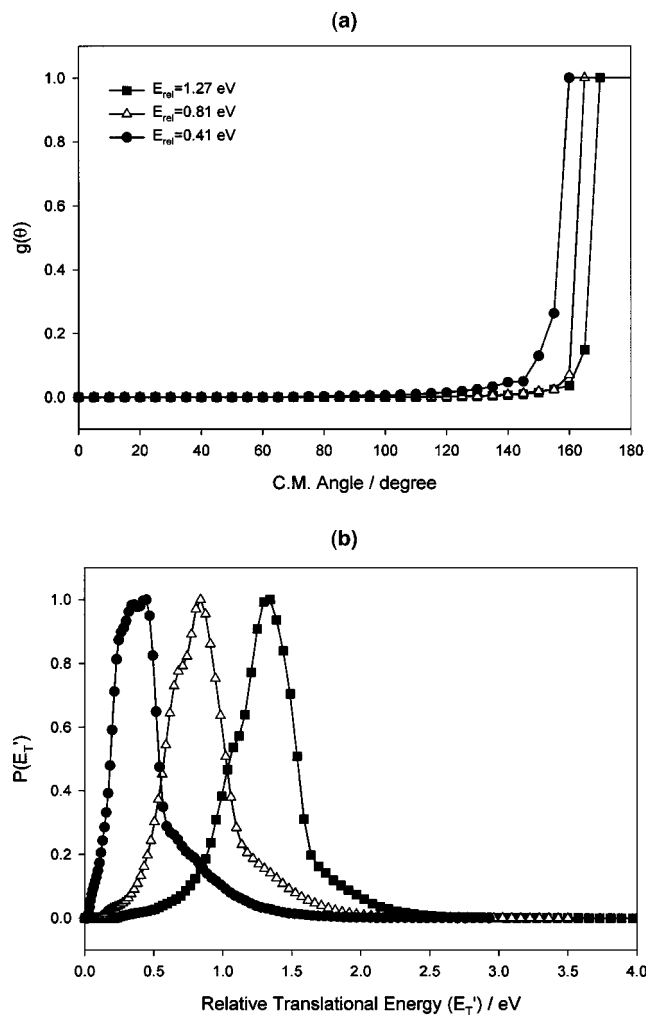


FIG. 4. (a) Center-of-mass angular distribution and (b) center-of-mass relative translational energy distribution of the product NH_4^+ ions at the three relative energies.

energy is increased, the relative translational energy of the products increases and the widths of the distribution slightly broaden. According to Fig. 4(b), the product average translational energies at the three energies are 0.47, 0.87, and 1.31 eV, respectively. The energy results of this study are listed in Table I. At the three collision energies studied, 23%, 35%, and 44% of the total energies are partitioned into the translational energies of the products, respectively. Thus the majority of the total energy is converted to the internal energy

TABLE I. Reaction energy results and RRKM rate constants at different relative energies (in eV).

Ion energy	0.74	1.61	2.57
Reactant relative energy E_T	0.41	0.81	1.27
Total energy E_{total}^a	2.09	2.50	2.95
Product relative energy E_T'	0.47	0.87	1.31
E_T'/E_{total}	23%	35%	44%
Product internal energy	1.62	1.63	1.65
E_{int}^*	2.99	3.39	3.85
k_{RRKM} (s^{-1})	3.3×10^{13}	4.2×10^{13}	5.3×10^{13}

^aCenter-of-mass energies. In order to transform to laboratory energies, $\mu V_c^2/2$ should be added, in which V_c is the center of mass velocity and μ is the reduced mass.

of the products. At the lowest collision energy of 0.41 eV, nearly 77% of the total energy appears in NH_4^+ internal excitation. However, almost 100% of the incremental translational energy in the two higher-energy experiments appears in product translational energy. Such an observation provides a classic example of “induced repulsive energy release.”^{28,29} Under such conditions, the small skew angle of the potential energy surface in mass-weighted coordinates³⁰ appropriate to the heavy+light-heavy mass combination of proton transfer facilitates trajectories that sample the corner of the surface where both the bonds being broken and formed are compressed. Under such circumstances, when the products are repelled into the exit valley, the incremental reactant translational energy converts mainly to product translational energy.

The proton transfer in Eq. (1) involves a fast motion of the proton from oxygen to nitrogen. If the proton is transferred while the nascent N–H bond is extended, it can be expected that the transfer process will mainly result in the excitation of the N–H bond stretching vibrations. However, the slight differences in the bond angles of NH_4^+ and NH_3 suggest that some of the reaction’s exothermicity may also be channeled into bending vibrations of NH_4^+ . Similarly, during proton transfer from oxygen to nitrogen, the geometry of the H_2O unit changes from C_{2v} to C_{3v} (Ref. 14) and can result in slight excitation of the H–O–H bending vibrations. The NH_4^+ ion is a polyatomic ion with nine vibrational frequencies, in which the N–H stretching mode vibrations are nondegenerate ν_1 (3236.6 cm^{-1}) and threefold degenerate ν_3 (3345.1 cm^{-1}).^{31,32} The results of this study cannot clearly assign which mode or both are excited. However, it should be noted that the energies of the two vibrational modes differ only by 0.013 eV. For visualization of the product energy disposal, we have superimposed on the Newton diagrams of Figs. 1–3 circles of constant barycentric speed corresponding to excitation of the ν_3 N–H stretching mode. As shown in Figs. 1–3, at the three collision energies, the product translational energy distributions are sharply peaked at barycentric speeds corresponding closely to NH_4^+ products internally excited with four quanta of N–H stretch. Viewed from the perspective of final NH_4^+ motion relative to incident NH_3 momentum, the sharply forward-peaked NH_4^+ angular distributions suggest that proton transfer occurs along a reaction coordinate of reduced dimensionality. Coupled with the high specificity for energy partitioning into product internal degrees of freedom, the reaction dynamics is consistent with proton transfer from H_3O^+ to NH_3 as the reactants approach, with the incipient N–H bond significantly extended from its equilibrium separation. Although the kinetic energy distributions alone are of insufficient information content to assign all product internal excitation to N–H stretching motion, long-distance proton transfer in the entrance channel is consistent with this simple picture.

Figure 4(b) provides additional evidence to support the picture of product internal excitation in N–H stretching motion. The figure shows that the relative translational energy distribution at 0.41 eV collision energy is asymmetric with a partially resolved “shoulder” appearing at about 0.8 eV. We attempted to fit the distribution using two Gaussian functions; the best fit was obtained using functions with the peak

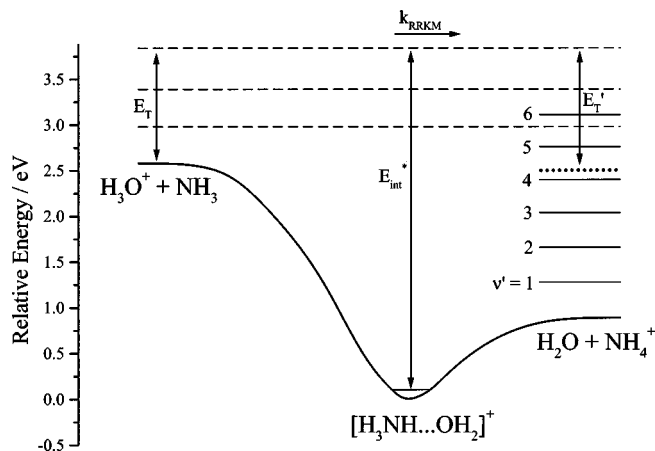


FIG. 5. Reaction energy diagram. Dashed line: the experimental collision energies. Dotted line: the product average recoil energy.

positions at 0.36 and 0.78 eV. The difference of the two peaks, 0.42 eV, is comparable to the 0.36 eV separation of N–H stretching vibrational energy levels. This nearly resolved structure in the kinetic energy distributions also suggests that energy partitioning selectively populates N–H stretches, with minimal rotational or bending vibrational excitation.

In the experiments, the neutral ammonia beam was generated by supersonic expansion; thus, most of the molecules are in the vibrational and rotational ground states. However, the protonated water ions were produced through a chemical ionization process in the electron impact source. The H_3O^+ ions produced in this manner are not completely vibrationally relaxed.³³ Thus, strictly, the total energies listed in Table I are only the lower limits.

The dissociation energy with the $\text{NH}_4^+ + \text{H}_2\text{O}$ channel of the $[\text{NH}_3\text{--H--H}_2\text{O}]^+$ complex has been determined to be 0.89 eV on the basis of the equilibrium measurements^{19–21} and theoretical calculations.^{11,15,16} Using the exothermicity for the proton transfer (1), the reaction coordinate diagram of Fig. 5 can be constructed. We performed density functional theory (DFT) calculations to obtain the vibrational frequencies of the $[\text{NH}_3\text{--H--H}_2\text{O}]^+$ complex required for Rice–Ramsperger–Kassel–Marcus (RRKM) lifetime calculations discussed later. The DFT calculations were performed using the GAUSSIAN 98 program package.³⁴ The $[\text{NH}_3\text{--H--H}_2\text{O}]^+$ ion structure was fully optimized at the B3LYP/6-31G(*d*) level and single-point energy calculations were done at the B3LYP/6-31G(*d*) and B3LYP/6-311+G(*d,p*) levels on the basis of the B3LYP/6-31G(*d*) geometries. The geometrical parameters of the $[\text{NH}_3\text{--H--H}_2\text{O}]^+$ complex are comparable with other theoretical results,^{11–18} and dissociation energies agree with previous work within 2%.

The kinematic analysis of the experimental data shows that the mean internal energy of the reaction products is 1.6 eV, independent of collision energy. This value is approximately 95% of the reaction exothermicity. With respect to the reaction coordinate diagram of Fig. 5, it is clear that the proton transfer process appears to conserve translational energy in the sense that the incident translational energy is transformed essentially quantitatively into product transla-

tional energy. The reaction exothermicity, which quantifies the increase in the strength of the newly formed N–H bond over that of the broken O–H bond, is transformed almost quantitatively into internal excitation of the nascent bond. This picture suggests that the proton transfers to NH_3 at long range, such that the incipient N–H bond is highly extended. At the transition state for proton transfer, reactive motion is along the N–H coordinate and the energy of the reaction is released as the reactants approach. These circumstances lead to a high level of N–H vibrational excitation in the products. The highly skewed nature of the potential energy surface³⁰ allows the breaking bonds and forming bonds to be compressed simultaneously, with efficient conversion of reactant translation into product translation. In the present case, with respect to the collision dynamics at the lowest relative energy, incremental translational energy appears essentially exclusively in the incremental translational energy of the products. This proton transfer system provides a paradigm for induced repulsive energy release.

The data demonstrate that the reaction is direct at all collision energies, but nevertheless reflect critical information about the dynamics of simultaneous bond breaking and bond making. This situation contrasts with the familiar spectator stripping model of direct reaction dynamics³⁵ in which, in the context of the present reaction, the H_2O product would serve as a “spectator” to the proton transfer process, with its center-of-mass speed unchanged from that of the incident H_3O^+ reactant. In fact, the spectator stripping model predicts that the reaction products would have much higher translational energies than are observed.

In an experimental study using the selected ion flow tube technique, Smith *et al.*²⁴ measured the rate coefficients and product ion distributions for the reactions between the $\text{H}_3\text{O}^+(\text{H}_2\text{O})_n$ and $\text{D}_3\text{O}^+(\text{D}_2\text{O})_n$ ($n=0–2$) ions and D_2O , H_2O , and NH_3 . For the D_2O and H_2O isotopic exchange reactions, they found that the distribution of H and D among the product ions and neutrals was purely statistical. Thus these reactions proceed via the formation of a long-lived intermediate, in which total randomization of the H and D atoms takes place prior to unimolecular dissociation. However, for the reaction between D_3O^+ and NH_3 , NH_3D^+ was found to be the only product ion and no appreciable isotopic exchange occurred. They suggested that the reaction proceeds via a simple mechanism and the intermediate complex has a short lifetime. Honma *et al.*²⁵ studied the reaction of protonated water clusters with deuterated ammonia using guided ion beam mass spectrometry. The authors did not observe the NH_2D_2^+ or DH_2O^+ ions, the H/D randomization products. They suggested that the reactions proceed via a direct proton transfer or via a relatively short-lived intermediate. The conclusions of these experiments are consistent with those of this study. However, in this study, the velocities and directions of the reactant H_3O^+ ion beam and the neutral NH_3 beam were better controlled, and the angular and kinetic energy distributions of the product NH_4^+ ion were precisely determined, providing direct evidence for an impulsive reaction mechanism.

The internal energy of the $[\text{NH}_3\text{--H--H}_2\text{O}]^+$ complex is

known; thus, we can estimate the lifetime of the complex using the RRKM theory formula^{36–39}

$$k(E) = \frac{\sigma N^\ddagger(E^* - E_0)}{h\rho(E^*)}, \quad (6)$$

in which E_0 is the activation energy, $N^\ddagger(E^* - E_0)$ is the sum of states of the transition state from 0 to $E^* - E_0$, and $\rho(E^*)$ is the density of states of the complex, respectively. σ is the symmetry parameter, which is 1 for the above dissociation reaction. As shown in Fig. 5, the internal energy of the $[\text{NH}_3\text{--H--H}_2\text{O}]^+$ complex is the sum of the collision energy and the dissociation energy of the $\text{H}_3\text{O}^+ + \text{NH}_3$ channel. The dissociation to $\text{H}_2\text{O} + \text{NH}_4^+$ is expected to be a direct process without a reverse activation energy barrier so that no unique transition state could be calculated. We thus approximated the transition state frequencies by calculating the frequencies of the $[\text{NH}_3\text{--H--H}_2\text{O}]^+$ structure with a (N)H–O bond length extended to 4.0 Å. This leads to an imaginary frequency corresponding to the stretching vibration of the H–O bond. As discussed by Li and Baer,⁴⁰ some adjustments for these estimated transition-state frequencies are necessary. In this study, the lowest five frequencies are arbitrarily scaled by a factor of 0.5. These lowest frequencies will convert to the rotational or translational degrees of freedom of the dissociation products. Using the transition-state frequencies, the activation entropy of the dissociation, $\Delta S_{600\text{ K}}^\ddagger$, is determined to be 28 J/mol K, a characteristic value of a reaction with a “loose” transition state. The RRKM calculations show that the unimolecular dissociation rate constant of the $[\text{NH}_3\text{--H--H}_2\text{O}]^+$ complex at the studied collision energies is about $3\text{--}5 \times 10^{13} \text{ s}^{-1}$. Thus the lifetime of the complex is just about 100 fs, 10 times longer than a N–H bond stretching vibrational period and two orders of magnitude shorter than the rotational period of the $[\text{NH}_3\text{--H--H}_2\text{O}]^+$ complex (about 20 ps according to the DFT calculated rotational constant, 7 GHz). We also tested the sensitivity of the calculated dissociation rate constant to the scaling factor for the five lowest frequencies by adjusting the factor from 0.8 to 0.3. These adjustments result in a $\Delta S_{600\text{ K}}^\ddagger$ of 8.5 J/mol K for 0.8 (49.1 J/mol K for 0.3); correspondingly, the dissociation rate constant becomes $4 \times 10^{12} \text{ s}^{-1}$ for 0.8 ($5 \times 10^{14} \text{ s}^{-1}$ for 0.3) at the relative energy of 0.41 eV. Thus the lifetime of the $[\text{NH}_3\text{--H--H}_2\text{O}]^+$ complex has a range from 5 to 600 fs, which although broad is below the rotational period of the complex. The above RRKM calculations support the conclusion that the $[\text{NH}_3\text{--H--H}_2\text{O}]^+$ complex is short lived in comparison with the rotational period of the complex. As discussed above, the internal energies of the $[\text{NH}_3\text{--H--H}_2\text{O}]^+$ complex in Table I are only lower limits; thus, the actual dissociation rate may be higher.

According to the RRKM calculations, if the $[\text{NH}_3\text{--H--H}_2\text{O}]^+$ complex has a lifetime of 20 ps, its maximum internal energy is 0.34 eV, even lower than the relative energy of the $\text{H}_3\text{O}^+ + \text{NH}_3$ channel. Thus it can be expected that no long-lived intermediate complex should be observed in the $\text{H}_3\text{O}^+ + \text{NH}_3$ reaction even using lower experimental collision energies.

Theoretically, a set of snapshots of the proton motion in the H_3O^+ and NH_3 system was obtained by Cheng²³ using

molecular dynamics simulations. In his study, the initial relative orientation of the two units was chosen randomly, the center-of-mass velocities were set to zero, and the N–O length was set to 8 a.u. He found that during the first 50 fs, the relative motion of the two species is slow and H_3O^+ rotates into a position in which one of the H atoms is directed toward NH_3 . At a N–O distance of 5.7 a.u. ($t=84$ fs), the velocity of the proton nearest to NH_3 increases suddenly and at $t=90\text{--}100$ fs the proton completely transfers to NH_3 . After the transfer process, the $[\text{NH}_3\text{--H--H}_2\text{O}]^+$ is vibrationally excited. Similar results are also obtained by Bueker *et al.*^{15,22} on the basis of the *ab initio* potential energy surface. They found that most of the excitation energy (about 80%) is in the vibration of the new N–H bond. As discussed above, this study shows that almost all the reaction exothermicity of the proton transfer is converted to the internal excitation of the NH_4^+ ions.

V. CONCLUSIONS

The crossed molecular beam technique is used to study the proton transfer dynamics between H_3O^+ and NH_3 . At the three experimental energies, the center-of-mass flux distributions of the product ion NH_4^+ exhibit sharply asymmetry, and the maxima are close to the velocity and direction of the precursor ammonia beam. The reaction transforms almost all of the 1.69 eV exothermicity into internal excitation of the products at all three collision energies. The increasing fraction of the reactant translational energy partitions into the translational energy of the products almost by 100%. This observation is consistent with the “induced repulsive energy release” mechanism. The RRKM calculations show that the lifetime of the intermediate complex $[\text{NH}_3\text{--H--H}_2\text{O}]^+$ is of magnitude 100 fs, two orders of magnitude shorter than the rotational period of the complex. The results indicate that the proton transfer reaction proceeds through a direct channel with large impact parameters.

ACKNOWLEDGMENTS

The authors express their appreciation to the U.S. Department of Energy for financial support. The authors are grateful for the assistance of Xiaohui Cai and Li Liu in the experiments of this work.

¹ *Proton Transfer Reactions*, edited by E. Caldin and V. Gold (Chapman and Hall, London, 1975).

² M. Rini, B.-Z. Magnes, E. Pines, and E. T. J. Nibbering, *Science* **301**, 349 (2003).

³ Y. Li, X. Liu, X. Wang, and N. Lou, *Chem. Phys. Lett.* **276**, 339 (1997).

⁴ M. Biczysko and Z. Latajka, *Chem. Phys. Lett.* **313**, 366 (1999).

⁵ S.-C. Park, K.-W. Maeng, T. Pradeep, and H. Kang, *Angew. Chem., Int. Ed. Engl.* **40**, 1497 (2001).

⁶ A. A. Viggiano, F. Dale, and J. F. Paulson, *J. Chem. Phys.* **88**, 2469 (1988).

⁷ P. W. Ryan, C. R. Blakley, M. L. Vestal, and J. H. Futrell, *J. Phys. Chem.* **84**, 561 (1980).

⁸ <http://webbook.nist.gov/chemistry/om/>

⁹ K. Y. Choo, H. Shinohara, and N. Nishi, *Chem. Phys. Lett.* **95**, 102 (1983).

¹⁰ H.-C. Chang, Y.-S. Wang, Y. T. Lee, and H.-C. Chang, *Int. J. Mass Spectrom. Ion Processes* **179/180**, 91 (1998).

- ¹¹J.-J. Delpuech, G. Serratrice, A. Strich, and A. Veillard, *Mol. Phys.* **29**, 849 (1975).
- ¹²L. Jaroszewski, B. Lesyng, and J. A. McCammon, *J. Mol. Struct.: THEOCHEM* **283**, 57 (1993).
- ¹³L. Jaroszewski, B. Lesyng, J. J. Tanner, and J. A. McCammon, *Chem. Phys. Lett.* **175**, 282 (1990).
- ¹⁴S. Roszak, U. Kaldor, D. A. Chapman, and J. J. Kaufman, *J. Phys. Chem.* **96**, 2123 (1992).
- ¹⁵H.-H. Bueker and E. Uggerud, *J. Phys. Chem.* **99**, 5945 (1995).
- ¹⁶C. A. Deakyne, *J. Phys. Chem.* **90**, 6625 (1986).
- ¹⁷S. Scheiner, *Int. J. Quantum Chem.* **23**, 753 (1983).
- ¹⁸S. Scheiner and L. B. Harding, *J. Phys. Chem.* **87**, 1145 (1983).
- ¹⁹M. Meot-ner (Mautner), *J. Am. Chem. Soc.* **106**, 1265 (1984).
- ²⁰J. D. Payzant, A. J. Cunningham, and P. Kebarle, *Can. J. Chem.* **51**, 3242 (1973).
- ²¹M. Meot-ner (Mautner) and C. V. Speller, *J. Phys. Chem.* **90**, 6616 (1986).
- ²²H.-H. Bueker, T. Helgaker, K. Ruud, and E. Uggerud, *J. Phys. Chem.* **100**, 15 388 (1996).
- ²³H.-P. Cheng, *J. Chem. Phys.* **105**, 6844 (1996).
- ²⁴D. Smith, N. G. Adams, and M. J. Henchman, *J. Chem. Phys.* **72**, 4951 (1980).
- ²⁵K. Honma, L. S. Sunderlin, and P. B. Armentrout, *Int. J. Mass Spectrom. Ion Processes* **117**, 237 (1992).
- ²⁶D. F. Varley, D. J. Levandier, and J. M. Farrar, *J. Chem. Phys.* **96**, 8806 (1992).
- ²⁷P. E. Siska, *J. Chem. Phys.* **59**, 6052 (1973).
- ²⁸*Dynamics of Molecular Collisions*, edited by W. H. Miller (Plenum, New York, 1976), Part B, Vol. 2.
- ²⁹A. M. G. Ding, L. J. Kirsch, D. S. Perry, J. C. Polanyi, and J. L. Schreiber, *Faraday Discuss. Chem. Soc.* **55**, 252 (1973).
- ³⁰J. O. Hirschfelder, *Int. J. Quantum Chem., Symp.* **3**, 17 (1969).
- ³¹J. M. L. Martin and T. J. Lee, *Chem. Phys. Lett.* **258**, 129 (1996).
- ³²Y. Yamaguchi and H. F. Schaefer III, *J. Chem. Phys.* **73**, 2310 (1980).
- ³³J. E. Moryl, W. R. Creasy, and J. M. Farrar, *J. Chem. Phys.* **82**, 2244 (1985).
- ³⁴M. J. Frisch, G. W. Trucks, H. B. Schlegel *et al.*, computer code, GAUSSIAN 98, A.11.1 ed., Gaussian, Inc., Pittsburgh, 2001.
- ³⁵A. Henglein, K. Lacmann, and G. Jacobs, *Ber. Bunsenges. Phys. Chem.* **69**, 279 (1965).
- ³⁶T. Baer and W. L. Hase, *Unimolecular Reaction Dynamics: Theory and Experiments* (Oxford University Press, New York, 1996).
- ³⁷L. S. Kassel, *J. Phys. Chem.* **32**, 225 (1928).
- ³⁸R. A. Marcus and O. K. Rice, *J. Phys. Colloid Chem.* **55**, 894 (1951).
- ³⁹O. K. Rice and H. C. Ramsperger, *J. Am. Chem. Soc.* **49**, 1617 (1927).
- ⁴⁰Y. Li and T. Baer, *J. Phys. Chem. A* **106**, 8658 (2002).